

Gene transcriptomic profile in arabis thaliana mediated by radiation-induced bystander effects

A. Yang¹, W. Xu², C. Deng², J. Wu², T. Wang^{2*}

¹School of Management, Hefei University of Technology, Hefei, P. R. China

²Key laboratory of high magnetic field and ion beam physical biology, Hefei institutes of physical science, Chinese Academy of Sciences, Hefei, P. R. China.

ABSTRACT

Background: The in vivo radiation-induced bystander effects (RIBE) at the developmental, genetic, and epigenetic levels have been well demonstrated using model plant *Arabidopsis thaliana* (*A. thaliana*). However, the mechanisms underlying RIBE in plants are not clear, especially lacking a comprehensive knowledge about the genes and biological pathways involved in the RIBE in plants. **Materials and Methods:** A high-density oligonucleotide probe-based cDNA microarray was used to analyze transcriptomic response in aerial leaf tissues of *A. thaliana* seedlings at 24 h after root exposure to 10 Gy of α -irradiation. **Results:** The root-localized irradiation resulted in up-regulated expressions of 238 genes and down-regulated expressions of 42 genes in bystander aerial tissues with a ≥ 2.0 -fold difference and < 0.05 p-values. The high frequency of gene families for up-regulated expressions were glutathione S-transferases, cytochrome P450 enzyme, the ethylene response factor, and the multidrug and toxic compound extrusion efflux, and for down-regulated expressions was the later embryogenesis abundant protein. Moreover, there were 200 up-regulated genes and 183 down-regulated genes with 1.5–2.0-fold expression changes. **Conclusion:** In addition to the canonical IR-induced genes, some genes that are not previously linked to radiobiological effects were found to be involved in RIBE in plants.

Keywords: Radiation-induced bystander effects, transcriptomic profile, cDNA microarray, *Arabidopsis thaliana*, α -particle irradiation.

► Original article

*Corresponding authors:

Wang Ting, PhD,

Fax: + 86 551 6559 5670

E-mail: wangting@ipp.ac.cn

Revised: February 2018

Accepted: November 2018

Int. J. Radiat. Res., July 2019;
17(3): 369-377

DOI: 10.18869/acadpub.ijrr.17.3.369

INTRODUCTION

The canonical radiation biology dogma describes the effects of ionizing radiation that are restricted to directly hit cells ⁽¹⁾. Radiation-induced bystander effects (RIBE), however, represent a paradigm shift in the understanding of the radiobiological effects, in which biological effects are induced in non-hit cells when their neighboring cells are irradiated ⁽²⁾. The RIBE have been well demonstrated in single-cell culture models ^(1, 3-5), multi-cellular tissue models ⁽⁶⁻¹¹⁾ and whole organisms ⁽¹²⁻¹⁹⁾.

Recently, the RIBE in model plant *Arabidopsis thaliana* (*A. thaliana*) have been well investigated in our research team ⁽²⁰⁻²⁸⁾. After

micro-beam irradiation of naked seed embryos and low-energy ion irradiation of intact seeds, some of the post-embryonic developmental phenotypes were significantly inhibited, which differentiate from the non-irradiated shoot apical meristem cells and root apical meristem cells ^(20, 21). We also demonstrated long-distance bystander mutagenic effects with root-irradiation in growing seedlings and dormant seeds of *A. thaliana*. The root-localized irradiation resulted in an enhanced level of DNA damage, which further promoted the activity of the homologous recombination repair machinery characterized by the up-regulation of the *AtRAD54* gene expression and an increased homologous recombination frequency ^(22, 23).

Some changes in DNA epigenetic status, such as DNA methylation and transcriptional gene silencing (TGS), were also observed in the RIBE in plants (28). In addition to the testing for various types of biological endpoints, the signal pathways of ROS (22, 24, 28) and Jasmonic acid (JA) (27, 29) have also been found to take part in the induction of RIBE. Although so, there is no yet a comprehensive knowledge about the molecular mechanisms underlying the RIBE in plants.

Transcriptomic profile can generate useful information about the differential expression of genes under various stress conditions (30), and can be analyzed using a high-throughput microarray that provides detailed information on a genome-wide scale with advantages in analysis speed, accuracy and comprehensiveness (31). Recently, the microarray for transcriptomic profile has been widely applied for plant researches (32). Here, we adopted the high-density oligonucleotide probe-based cDNA microarray to profile gene expressions in the bystander aerial tissues of *A. thaliana* seedlings after root exposure to α -irradiation. The resulting data from gene transcript arrays were further analyzed on multiple levels, including distribution and extent of transcriptional changes, the significance of gene up-regulation, the high frequency gene families, biological processes, and pathways.

MATERIALS AND METHODS

A. thaliana Lines and Plant Growth

The wild-type *A. thaliana* line (Columbia ecotype) was obtained from the NASC (Nottingham Arabidopsis Stock Center, UK).

A. thaliana seeds were soaked in water and incubated in the dark at 4°C for two days before they were sown on growth medium (1× Murashige and Skoog (MS) mineral salts, 0.8% agar [w/v], and 1% sucrose [w/v]) in square petri dishes that were then placed in a growth chamber in a vertical orientation. The growth chamber was maintained at 22°C, with an illumination of approximately 100 $\mu\text{M m}^2\text{s}^{-1}$ and a 16-h light/8-h dark cycle.

Root-Localized Irradiation with α -Particles

α -particles emitted from a ^{241}Am source with an activity of 7.4 MBq in the Rotate-Adjustable α -particle Source Facility. Root-localized irradiation of *A. thaliana* was performed as described previously (22), and is also shown schematically in figure 1. In the present study, the 7-day-old seedlings were used for root exposure to α - particles. The average energy of α - particles measured 3.3 MeV, and the particles were delivered at a dose rate of α -particles of 1.51 cGys⁻¹.

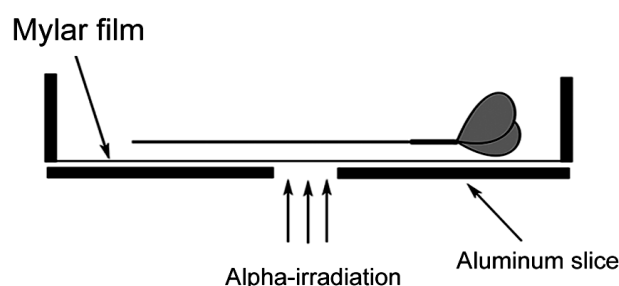


Figure 1. Schematics of the root-localized irradiation of *A. thaliana* with α -particles.

Microarray Analysis

Three control groups (N1-N3) and three irradiated groups (P1-P3) were sampled and frozen in liquid nitrogen at 24 h after root irradiation, and total RNA from aerial tissues was extracted using the Trizol reagent (Invitrogen, Thermo Fisher Scientific, Waltham, MA, USA). The quantity and quality of isolated total RNA were assessed by spectrophotometry and gel electrophoresis, respectively. All the microarray experiments were performed using Agilent *Arabidopsis* (V4; 4 × 44k) microarrays by CapitalBio Corp. (CapitalBio Corp., Beijing, China). Microarrays were scanned with a LuxScan™ 10K confocal laser scanner (CapitalBio Corp.), and the resulting images were analyzed with SpotData software (CapitalBio Corp.). Spots with fewer than 50% of the signal pixels that exceeded the local background value for both channels (Cy3 and Cy5), plus two standard deviations of the local background, were removed from the analysis. This step further ensured that spots with characteristic doughnut shapes that are

often encountered on microarrays would not be part of the subsequent analysis. An intensity-dependent program (LOWESS) in the R language package was used to normalize the ratio values. Identification of differentially expressed genes and determination of statistical significance were performed using GeneSpring GX software (Agilent Technologies Inc, Santa Clara, CA, USA). These genes were cluster analyzed using the Cluster 3.0 software (University of Tokyo, Tokyo, Japan). Genes that had ≥ 2 -fold expression change (P -value < 0.05) and that were annotated in the TAIR database were selected for Gene ontology (GO) analysis and pathway analysis using the Molecule Annotation System (CB-MAS_3.0, <http://bioinfo.capitalbio.com/mas3/>).

Real-time PCR analysis

The total RNAs were extracted using the Trizol reagent (Invitrogen, USA) according to manufacturer's protocols 24 h after root-localized irradiation. Total RNA was reverse transcribed using Transcript One-Step gDNA removal and the cDNA synthesis Supermix kit (Transgen Biotech, China) according to

manufacturer's protocols. The qRT-PCR was conducted with the ABI StepOne plus system (Applied Biosystemst, Carlsbad, CA) according to the manufacturer's instructions. Each PCR reaction (20 μ l) contained 10 μ l 2 \times real-time PCR Mix, 0.2 μ M of each primer and cDNA. The qRT-PCR was performed under the following conditions: 95°C for 10 sec for one cycle; 95°C for 15 sec, 60°C for 30 sec, 72°C for 30 sec for 40 cycles. The primers used are listed in table 1, which also indicated that the *ACTIN2* gene was used as an internal control. The final data were compiled as the average of three independent experiments, with three technical replicates for each experiment. The statistical significance between control and irradiated groups was analyzed using the Origin 7.5 software (OriginLab Corporation, Northampton, MA, USA).

Statistical analysis

All the results are presented as mean \pm standard deviation. The statistical significance of the experiments was determined by performing student's *t* test. A P -value of 0.05 or less was considered significant.

Table 1. qRT-PCR primer sequences used for validation of the microarray analysis.

| | |
|-------------|-------------------------------|
| PXMT1-F | 5'-CAGCGCTGGAGTTCCTGGTT-3' |
| PXMT1-R | 5'-CCCGTGCACTGCATGTCTTT-3' |
| AtGSTU9-F | 5'-GGTGAACCAACTGTGACGAACG-3' |
| AtGSTU9-R | 5'-TCCACCCGTAGACACCAGGAA-3' |
| AT2G04050-F | 5'-ATGGGGTTGCAAGGGGAAGT-3' |
| AT2G04050-R | 5'-TCCGACCACAACACCACACC-3' |
| CYP710A1-F | 5'-TGTTGCGCGAGGATCACAAA-3' |
| CYP710A1-R | 5'-ACGGACAAGCTGTCGAGTG-3' |
| ABR1-F | 5'-TTGGCTCGGTACGTTTCGACA-3' |
| ABR1-R | 5'-AGCGGTTTGGTGCACAGGTT-3' |
| LEA7-F | 5'-TGTTTGTGCGTTCGTGAGG-3' |
| LEA7-R | 5'-TGTAATTCCGTACTAATCACCCG-3' |
| AT3G21460-F | 5'-TTACGAGCAAGGTGTGAGCC-3' |
| AT3G21460-R | 5'-AACAAAAACCGCAGGAACCG-3' |
| ACTIN2-F | 5'-CTAAGCTCTCAAGATCAAAGGC-3' |
| ACTIN2-R | 5'-AACATTGCAAAGAGTTTCAAGG-3' |

RESULTS

Microarray-based expression profile

After the microarray experiment, a hierarchical cluster analysis was performed for these genes with ≥ 2 -fold expression changes ($P < 0.05$). As shown in figure 2, In this map 238 genes were listed for up-regulated expression and 42 genes for down-regulated expression (figure 2). Next, these listed genes were further sorted according to the extent of their fold changes. Fold changes in up-regulated and down-regulated genes were represented by positive and negative numbers, respectively. As shown in figure 3, nearly half of the genes (132 genes) had 2- to 3-fold up-regulated expressions, and expressions of 18 genes increased by more than 7-fold. In contrast, only 42 genes were down-regulated by the root irradiation (≥ 2 -fold change), most of which (28 genes) had 2- to 3-fold changes. It is worth noting that the RIBE are typical weak radiation responses, therefore, the genes whose expression changes between 1.5- and 2-fold should also be considered in RIBE. According to this judgment, there were additional 200 up-regulated genes and 183 of down-regulated genes. These results suggest that RIBE might mediate an extensive gene expression changes.

Validation of microarray results by qRT-PCR analysis

To confirm the microarray results, the up-regulated *AtGSTU9*, *AT2G04050*, *ABR1*, *CYP710A1*, and *PXMT1* genes and down-regulated *LEA7* and *AT3G21460* genes were representatively chosen for qRT-PCR analysis. As shown in figure 4, the expression patterns for all tested genes were coincident with the data in microarray analysis although the fold changes were different. The microarray analysis showed that the fold change was 17 for *AtGSTU9*, 13 for *At2G04050*, 6.5 for *ABR1*, 8 for *CYP710A1*, and 5.8 for *PXMT1*, whereas their fold changes in qRT-PCR analysis were 4.3, 3.4, 6.5, 4.1, and 1.6 compared to the controls, respectively. The fold changes in microarray analysis were 8.4 for *LEA7* and 5.3 for *AT3G21460*, whereas their fold changes in

qRT-PCR analysis were 1.8 and 9.5 compared to the control groups, respectively. The differences might mainly be due to the different signal extraction and comparative methods between microarray and qRT-PCR analysis⁽³³⁾.

Gene families, biological processes, and biological pathways involved in RIBE

Fourteen of highly inducible genes included the *AT5G55150* (25.34-fold), *AT5G62480* (*ATGSTU9*) (17.69), *AT2G04050* (13.71), *AT2G34500* (*CYP710A1*) (13.55), *AT1G13340* (11.64), *AT3G22231*(*PCCT1*) (11.43), *AT2G38823* (10.99), *AT1G32350*(*AOX1D*) (10.26), *AT3G49540* (10.22), *AT5G01380* (9.09), *AT5G24640* (8.51), *AT3G54530* (8.12), *AT1G66700*(*PXMT1*) (7.93), and *AT3G19615* (7.58). Among them, the biological function of the highest induced *AT5G55150* gene was not yet characterized, and the second is the gene of Glutathione transferase (GSTs), and the fourth was the gene of C22-sterol desaturase, suggesting an involvement of oxidative stress responses in RIBE. We further classified the genes with ≥ 2 -fold expression changes into different families. As shown in table 2, 12 of the up-regulated genes belong to GST family, accounting for 5.1% of total up-regulated genes identified in the microarray analysis. Other up-regulated genes are the members of the cytochrome P450 enzyme family⁽⁵⁾, ethylene response factor (ERF) subfamily⁽³⁾ and MATE efflux family⁽³⁾, respectively. Moreover, five down-regulated genes were from the Later Embryogenesis Abundant protein (LEA) family, which account for 11.9% of total down-regulated genes. These results suggest that these gene families might be involved in the RIBE.

We further sorted out these inducible and repressive genes based on their annotated biological processes. These genes were distributed into 10 biological process groups, most of which correlate with oxidative stress responses (table 3). Of these 28 genes were associated with oxidation reduction and 14 with oxidative stress. They were further clustered into six biological pathways, as shown in table 3.

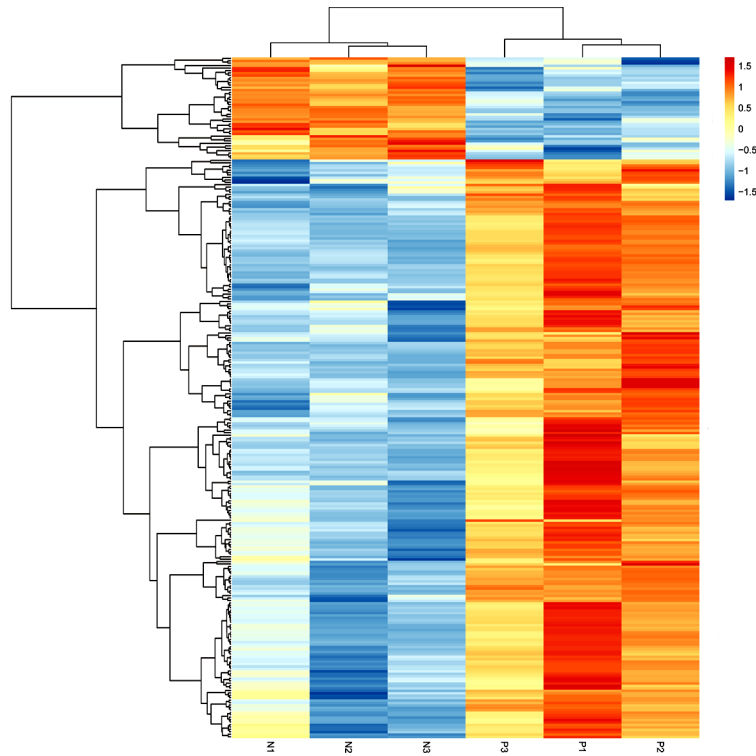


Figure 2. Hierarchical cluster analysis of 280 genes with > 2-fold expression change. Each horizontal line represents the expression data for one gene in aerial plant tissues from control and root-irradiated aerial plants. Colors show the normalized expression level. Induction (or repression) ranges from white to red (or blue) with a fold-change scale bar shown on the right of cluster. N1-N3: control groups, P1-P3: irradiated groups.

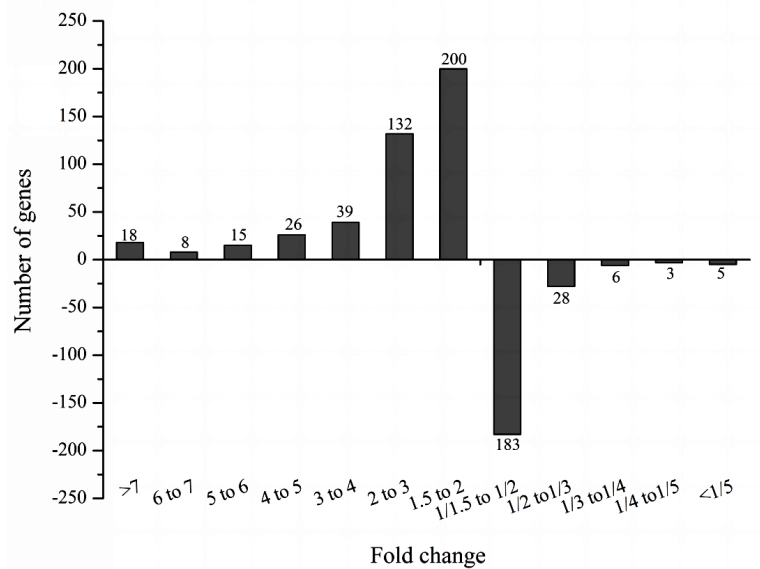


Figure 3. The number of RIBE-mediated genes with different fold changes, and the numbers above the column represent the number of genes with the specific fold changes.

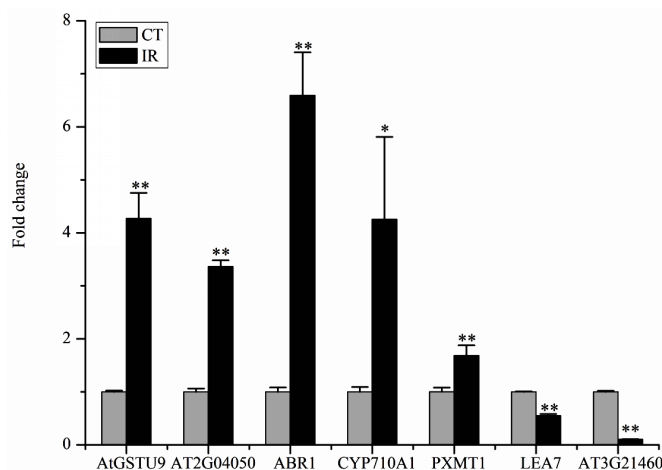


Figure 4. qRT-PCR analysis of 7 representative genes. These genes were selected from the significantly up-regulated or down-regulated gene groups for validation of the microarray analysis. Results are expressed as the means \pm SD (n=3, t test * P<0.05 and ** P < 0.01).

Table 2. The high frequency of gene families involved in RIBE.

| Gene family | Gene | Fold change | regulation |
|--|-----------|-------------|------------|
| GSTs | ATGSTU9 | 17.68889 | up |
| | ATGSTL1 | 5.962991 | up |
| | ATGSTU25 | 4.605921 | up |
| | ATGSTU11 | 4.441361 | up |
| | ATGSTF6 | 3.820138 | up |
| | ATGSTF2 | 3.350726 | up |
| | ATGSTU4 | 3.16003 | up |
| | ATGSTF3 | 3.107264 | up |
| | ATGSTF7 | 2.694439 | up |
| | ATGSTF12 | 2.399328 | up |
| | ATGSTF9 | 2.327342 | up |
| ATGSTF11 | 2.073808 | up | |
| Cytochrome P450 enzyme | CYP710A1 | 13.546226 | up |
| | CYP76C2 | 5.886769 | up |
| | PAD3 | 5.855027 | up |
| | CYP79F1 | 2.956539 | up |
| | CYP83A1 | 2.118532 | up |
| MATE efflux family protein | AT2G04050 | 13.71277 | up |
| | AT2G04066 | 3.94306 | up |
| | AT2G04070 | 3.086136 | up |
| ERF (ethylene response factor) subfamily | ABR1 | 6.540907 | up |
| | AT2G47520 | 4.83663 | up |
| | AT5G13330 | 2.129644 | up |
| Late embryogenesis abundant protein (LEA) family protein | AT1G52690 | 8.352396 | down |
| | AT3G17520 | 4.750286 | down |
| | AT5G06760 | 3.013772 | down |
| | AT3G02480 | 2.796134 | down |
| | AT2G41280 | 2.005858 | down |

Table 3. Gene ontology analysis of the biological processes and pathways involved in RIBE. p-value is the probability of seeing at least x (count) differential expression gene out of the total genes in the list annotated to a particular term. The q-value is the adjusted p-values found using an optimized FDR approach.

| Biological processes (GO Term) | Count | p-Value | q-Value |
|--|-------|----------|----------|
| GO:0009407 toxin catabolism | 13 | 1.78E-20 | 3.35E-18 |
| GO:0055114 oxidation reduction | 28 | 6.1E-13 | 3.82E-11 |
| GO:0006979 response to oxidative stress | 14 | 2.36E-11 | 1.11E-09 |
| GO:0009098 leucine biosynthesis | 5 | 1.48E-09 | 5.57E-08 |
| GO:0019761 glucosinolate biosynthesis | 5 | 1.93E-07 | 5.19E-06 |
| GO:0009414 response to water deprivation | 6 | 8.73E-05 | 0.001263 |
| GO:0009768 photosynthesis, light harvesting in photosystem I | 2 | 0.000143 | 0.00192 |
| GO:0007568 aging | 4 | 0.0002 | 0.002198 |
| GO:0042631 cellular response to water deprivation | 2 | 0.000214 | 0.002198 |
| GO:0009737 response to abscisic acid stimulus | 7 | 0.000222 | 0.002198 |
| Biological Pathways | | | |
| Metabolism of xenobiotics by cytochrome P450 | 5 | 7.04E-13 | 9.24E-13 |
| Drug metabolism - cytochrome P450 | 5 | 9.24E-13 | 9.24E-13 |
| Glutathione metabolism | 5 | 1.17E-10 | 7.78E-11 |
| Valine, leucine and isoleucine biosynthesis | 3 | 8.26E-07 | 4.13E-07 |
| Phenylpropanoid biosynthesis | 3 | 0.000119 | 4.78E-05 |
| Naphthalene and anthracene degradation | 2 | 0.000677 | 0.00018 |

DISCUSSION

In this study, we analyzed the genome-wide responses of *A. thaliana* to RIBE based on the microarray-based transcriptomic profile. It is well known that unlike irradiation-targeted effects, RIBE consist of production of bystander signals in the hit tissues (cells) and irradiation responses in non-hit bystander tissues (cells). In the experiments of the root-localized irradiation, due to the low-penetration potential of α -particles, the root cells directly traversed by α -particles cannot be accurately defined and separated from the naïve root cells. Therefore, in this study we only investigated the transcriptomic responses in bystander aerial tissues. Interestingly, a γ -induced transcriptomic profiles in aerial leaf tissues of *A. thaliana* has been reported⁽³³⁾. Comparing to the transcriptomic profiles in directly irradiated tissues in the work by Kim et al, we found that gene expressions in two irradiation patterns were completely different, and the direct irradiation leads to more than 3000 differentially expressed genes over 280 genes by the RIBE. This definitely indicates that the RIBE are weak radiobiological response relative to the direct radiation effects. However, in these two experiments, the differences in radiation quality (α -particles versus γ -rays) and radiation doses (10 Gy versus 200 Gy) also attenuated the reasonability of the comparison. Therefore, further experiments for comparing the transcriptomic responses in directly irradiated and bystander plant tissues should be carried out under the same irradiation conditions.

It has been reported that ROS play a pivotal role in mediating RIBE in plants^(22, 24, 28), in accordance with the up-regulated gene expressions of P450 family in the microarray analysis, in which five family members and two pathways were activated (tables 2, 3). Considering the role of P450 in oxidation of various substrates⁽³⁴⁾, they might mainly contribute the oxidative stress in bystander aerial tissues. The cells can accordingly initiate antioxidant mechanisms to eliminate the oxidative stress. It has been reported that GST family takes part in this process⁽³⁵⁾, and the

microarray analysis also showed that 12 genes of this family were highly inducible (table 2). In *A. thaliana*, the GST family contains 97 members that are organized into seven classes: *phi* (*GSTF*), *tau* (*GSTU*), *zeta* (*GSTZ*), *theta* (*GSTT*), *lambda* (*GSTL*), *dehydroascorbate reductase* (*DHAR*) and *tetrachloro-p-hydroquinone dehydrogenase-related* (*TCHQD*)⁽³⁶⁻³⁸⁾. In the present study, four *tau* genes and seven *phi* genes were found among the activated GST genes, indicating that the *GSTU* and *GSTF* were two important GST sub-families in the RIBE.

The microarray analysis also provided some new clues about the irradiation responses in bystander aerial tissues, such as the up-regulated expressions of *ERF* genes and the down-regulated expressions of the *Late Embryogenesis Abundant protein* (*LEA*) family. It is well accepted that the plant hormone ethylene is a regulator of a variety of developmental and stress responses in plants⁽³⁹⁾. However, there is no yet evidence about its involvement in RIBE. Moreover, it has been reported that the acquisition of desiccation tolerance during the late stages of seed development is correlated with the induction of *LEA* proteins⁽⁴⁰⁾. The *LEA* genes usually function in the late stages of seed development and their down-regulation in RIBE is hard to explain. We speculate that the RIBE might disturb plant development, leading to repressed expressions of *LEA* genes as a secondary reaction to plant development arrest.

In addition to these genes with > 2-fold expression change, the genes with 1.5- to 2-fold expression change should also be included in the RIBE, mainly considering that the RIBE are weak radiobiological responses relative to the radiation-targeted effects. In our previous studies, the DNA repair genes and TGS-silenced genes were definitely up-regulated in the bystander aerial tissues^(22, 28). Their expression changes were between 1.5- and 2-fold in the microarray analysis. With the judgment of 1.5–2-fold change, there were 200 up-regulated and 183 down-regulated genes. The deeper exploration to these genes might provide more insights into the mechanisms underlying the RIBE.

ACKNOWLEDGEMENT

We thank NASC for providing the *A. thaliana* seeds. This work was supported by the National Science Fund of China (11575233) and the Youth Innovation Promotion Association of Chinese Academy of Sciences (No. 2017485).

Conflicts of interest: Declared none.

REFERENCES

- Little JB (2000) Radiation carcinogenesis. *Carcinogenesis*, **21**: 397–404.
- Hei TK (2006) Cyclooxygenase-2 as a signaling molecule in radiation-induced bystander effect. *Mol Carcinog*, **45**: 455–460.
- Morgan WF (2003) Non-targeted and delayed effects of exposure to ionizing radiation: I. Radiation induced genomic instability and bystander effects in vitro. *Radiat Res*, **159**: 567–80.
- Mothersill C and Seymour CB (2004) Radiation-induced bystander effects— implications for cancer. *Nat Rev Cancer* **4**: 158–64.
- Hamada N, Matsumoto H, Hara T, Kobayashi Y (2007) Intercellular and intracellular signaling pathways mediating ionizing radiation-induced bystander effects. *Radiat Res*, **48**: 87–95.
- Belyakov OV, Folkard M, Mothersill C, Prise KM, Michael BD (2002) Bystander-induced apoptosis and premature differentiation in primary urothelial explants after charged particle microbeam irradiation. *Radiat Prot Dosimetry*, **99**:249–51.
- Belyakov OV, Folkard M, Mothersill C, Prise KM, Michael BD (2003) A proliferation-dependent bystander effect in primary porcine and human urothelial explants in response to targeted irradiation. *Br J Cancer*, **88**: 767–74.
- Belyakov OV, Mitchell SA, Parikh D, Randers-Pehrson G, Marino SA, Amundson SA, Geard CR, Brenner DJ (2005) Biological effects in unirradiated human tissue induced by radiation damage up to 1 mm away. *Proc Natl Acad Sci, USA* **102**: 14203–8.
- Belyakov OV, Folkard M, Mothersill C, Prise KM, Michael BD (2006) Bystander induced differentiation: a major response to targeted irradiation of a urothelial explant model. *Mutat Res*, **597**: 43–9.
- Persaud R, Zhou H, Baker SE, Hei TK, Hall EJ (2005) Assessment of low linear energy transfer radiation-induced bystander mutagenesis in a three-dimensional culture model. *Cancer Res*, **65**: 9876–82.
- Sedelnikova OA, Nakamural A, Kovalchuk O, Koturbash I, Mitchell SA, Marino SA, Brenner DJ, Bonner WM (2007) DNA double-strand breaks form in bystander cells after microbeam irradiation of three-dimensional human tissue models. *Cancer Res*, **67**: 4295–302.
- Watson GE, Lorimore SA, Macdonald DA, Wright EG (2000) Chromosomal instability in unirradiated cells induced *in vivo* by a bystander effect of ionizing radiation. *Cancer Res*, **60**: 5608–11.
- Xue LY, Butler NJ, Makrigiorgos GM, Adelstein SJ, Kassis AI (2002) Bystander effect produced by radiolabeled tumor cells *in vivo*. *Proc Natl Acad Sci, USA* **99**: 13765–70.
- Koturbash I, Rugo RE, Hendricks CA, Loree J, Thibault B, Kutanzi K, Pogribny I, Yanch JC, Engelward BP, Kovalchuk O (2006) Irradiation induces DNA damage and modulates epigenetic effectors in distant bystander tissue *in vivo*. *Oncogene*, **25**: 4267–75.
- Koturbash I, Boyko A, Rodriguez-Juarez R, McDonald RJ, Tryndyak VP, Kovalchuk I, Pogribny IP, Kovalchuk O (2007) Role of epigenetic effectors in maintenance of the long-term persistent bystander effect in spleen *in vivo*. *Carcinogenesis*, **28**: 1831–8.
- Koturbash I, Kutanzi K, Hendrickson K, Rodriguez-Juarez R, Kogosov D, Kovalchuk O (2008) Radiation-induced bystander effects *in vivo* are sex specific. *Mutat Res*, **642**: 28–36.
- Mancuso M, Pasquali E, Leonardi S, Tanori M, Rebessi S, Di Majo V, Pazzaglia S, Toni MP, Pimpinella M, Covelli V, Saran A (2008) Oncogenic bystander radiation effects in Patched heterozygous mouse cerebellum. *Proc Natl Acad Sci, USA* **105**: 12445–50.
- Bertucci A, Pocock RD, Randers-Pehrson G, Brenner DJ (2009) Microbeam irradiation of the *C. elegans* nematode. *J Radiat Res*, **50**: A49–A54.
- Guo X, Sun J, Bian P, Chen L, Zhan F, Wang J, Xu A, Wang Y, Hei TK, Wu L (2013) Radiation-induced bystander signaling from somatic cells to germ cells in *Caenorhabditis elegans*. *Radiat Res*, **180**: 268–275.
- Yang G, Wu L, Chen L, Pei B, Wang Y, Zhan F, Wu Y, Yu Z (2007) Targeted irradiation of shoot apical meristem of *Arabidopsis* embryos induces long-distance bystander/abscopal effects. *Radiat Res*, **167**: 298–305.
- Yang G, Mei T, Yuan H, Zhang W, Chen L, Xue J, Wu L, Wang Y (2008) Bystander/abscopal effects induced by low-energy ion irradiation on intact *Arabidopsis* seeds. *Radiat Res*, **170**: 372–80.
- Li F, Liu P, Wang T, Bian P, Wu Y, Wu L, Yu Z (2010) The induction of bystander mutagenic effects *in vivo* by a-irradiation in whole *Arabidopsis thaliana* plants. *Radiat Res* **174**:228–37.
- Li F, Wang T, Xu S, Yuan H, Bian P, Wu Y, Wu L, Yu Z (2011) Abscopal mutagenic effect of low-energy-ions in *Arabidopsis thaliana* seeds. *Int J Radiat Biol*, **87**: 1–10.
- Wang T, Li F, Xu S, Bian P, Wu Y, Wu L, Yu Z (2011) The time course of long-distance signaling in radiation-induced bystander effect *in vivo* in *Arabidopsis thaliana* demonstrated using root micro-grafting. *Radiat Res*, **176**: 234–43.
- Wang T, Li F, Xu W, Bian P, Wu Y, Wu L (2012) Novel features of radiation-induced bystander signaling in *Ara-*

- bidopsis thaliana* demonstrated using root micro-grafting. *Plant Signal Behav*, **7**: 1566–72.
26. Wang T, Sun Q, Xu W, Li F, Li H, Lu J, Wu L, Wu Y, Liu M, Bian P (2015) Modulation of modeled microgravity on radiation-induced bystander effects in *Arabidopsis thaliana*. *Mutat Res*, **773**: 27–36.
 27. Wang T, Xu W, Deng C, Xu S, Li F, Wu Y, Wu L, Bian P (2016) A pivotal role of the jasmonic acid signal pathway in mediating radiation-induced bystander effects in *Arabidopsis thaliana*. *Mutat Res*, **791**: 1–9.
 28. Xu W, Wang T, Xu S, Xu S, Wu L, Wu Y, Bian P (2015) Radiation-induced epigenetic bystander effects demonstrated in *Arabidopsis thaliana*. *Radiat Res*, **183**: 511–24.
 29. Xu W, Wang T, Xu S, Li F, Deng C, Wu L, Wu Y, Bian P (2016) UV-C-induced alleviation of transcriptional gene silencing through plant-plant communication: Key roles of jasmonic acid and salicylic acid pathways. *Mutat Res*, **790**: 56–67.
 30. Zhang T, Tang J, Sun J, Yu C, Liu Z, Chen J (2015) Hex1 related transcriptome of *Trichoderma atroviride* reveals expression patterns of ABC transporters associated with tolerance to dichlorvos. *Biotechnol Lett*, **37**: 1421–1429.
 31. Brandl J and Anderson MR (2015) Current state of genome-scale modeling in filamentous fungi. *Biotechnol Lett*, **37**: 1131–1139.
 32. Gul A, Ahad A, Akhtar S, Ahmad Z, Rashid B, Husnain T (2016) Microarray: gateway to unravel the mystery of abiotic stresses in plants. *Biotechnol Lett*, **38**: 527–543.
 33. Kim JH, Moon YR, Kim JS, Oh MH, Lee JW, Chung BY (2007) Transcriptomic profile of *Arabidopsis* rosette leaves during the reproductive stage after exposure to ionizing radiation. *Radiat Res*, **168**: 267–280.
 34. Mao G, Seebeck T, Schrenker D, Yu O (2013) CYP709B3, a cytochrome P450 monooxygenase gene involved in salt tolerance in *Arabidopsis thaliana*. *BMC Plant Biology*, **13**: 169.
 35. Sappl PG, Carroll AJ, Clifton R, Lister R, Whelan J, Millar AH, Singh KB (2009) The *Arabidopsis* glutathione transferase gene family displays complex stress regulation and co-silencing multiple genes results in altered metabolic sensitivity to oxidative stress. *Plant J*, **58**: 53–68.
 36. Sappl PG, Oñate-Sánchez L, Singh BK, Millar HA (2004) Proteomic analysis of glutathione S-transferases of *Arabidopsis thaliana* reveals differential salicylic acid-induced expression of the plant-specific phi and tau classes. *Plant Mol Biol*, **54**: 205–219.
 37. Dixon DP, Laphorn A, Edwards R (2002) Plant glutathione transferases. *Genome Biol*, **3**: 3004.1–3004.10.
 38. Dixon DP, Davis BG, Edwards R (2002) Functional divergence in the glutathione transferase superfamily in plants. Identification of two classes with putative functions in redox homeostasis in *Arabidopsis thaliana*. *J Biol Chem*, **277**: 30859–30869.
 39. Alonso JM, Hirayama T, Roman G, Nourizadeh S, Ecker JR (1999) EIN2, a bifunctional transducer of ethylene and stress responses in *Arabidopsis*. *Science*, **284**: 2148–2152.
 40. Dure L III, Crouch M, Harada J, Ho T-HD, Mundy J, Quatrano R, Thomas T, Sung ZR (1989) Common amino acid sequence domains among the LEA proteins of higher plants. *Plant Mol Biol*, **12**: 475–486.

